Development 133, 1789-1797 (2006) doi:10.1242/dev.02320

Twinstar, the *Drosophila* homolog of cofilin/ADF, is required for planar cell polarity patterning

Adrienne Blair[1], Andrew Tomlinson[2], Hung Pham[1], Kristin C. Gunsalus[3,*], Michael L. Goldberg[3] and Frank A. Laski[1,†]

Planar cell polarity (PCP) is a level of tissue organization in which cells adopt a uniform orientation within the plane of an epithelium. The process of tissue polarization is likely to be initiated by an extracellular gradient. Thus, determining how cells decode and convert this graded information into subcellular asymmetries is key to determining how cells direct the reorganization of the cytoskeleton to produce uniformly oriented structures. Twinstar (Tsr), the *Drosophila* homolog of Cofilin/ADF (actin depolymerization factor), is a component of the cytoskeleton that regulates actin dynamics. We show here that various alleles of *tsr* produce PCP defects in the wing, eye and several other epithelia. In wings mutant for *tsr*, Frizzled (Fz) and Flamingo (Fmi) proteins do not properly localize to the proximodistal boundaries of cells. The correct asymmetric localization of these proteins instructs the actin cytoskeleton to produce one actin-rich wing hair at the distal-most vertex of each cell. These results argue that actin remodeling is not only required in the manufacture of wing hairs, but also in the PCP read-out that directs where a wing hair will be secreted.

KEY WORDS: ADF/cofilin, Twinstar, Planar cell polarity, Lim Kinase, Frizzled, Flamingo, *Drosophila*

INTRODUCTION

Remodeling of the cytoskeleton is crucially required for various forms of cellular locomotion, such as chemotaxis and axon growth cone guidance. In these examples, the cellular architecture becomes differentially polarized in response to extracellular gradients of signaling molecules. How extracellular information is decoded by cells and used to direct the appropriate cytoskeletal polarization is currently the focus of intense study. A similar polarization mechanism occurs during the establishment of planar cell polarity (PCP), in which cells adopt a uniform orientation within the plane of an epithelium (Adler, 2002; Gubb and Garcia-Bellido, 1982; Uemura and Shimada, 2003). PCP is found throughout the metazoa, but is made particularly obvious in the fly wing as the outgrowth of single hairs from the distal-most vertices of cells, all collectively pointing towards the distal end of the wing (Wong and Adler, 1993). The wing is thus decorated with a multitude of hairs with the same orientation. PCP is evident in many other tissues of the fly, including the eye, where it is manifest not from the projections from single cells, but rather in the arrangement of a group of cells, the ommatidium (Wehrli and Tomlinson, 1995; Zheng et al., 1995) (Fig. 1A).

The PCP signal has been suggested to be a gradient of one or more extracellular ligands that is read by Frizzled (Fz), a serpentine receptor (Krasnow and Adler, 1994; Vinson and Adler, 1987; Vinson et al., 1989), which then regulates the cellular redistribution of itself and other core group PCP proteins that include: Disheveled (Dsh) (Axelrod, 2001; Krasnow et al., 1995), a cytoplasmic protein; Flamingo (Fmi), a cadherin also known as Starry Night (Stan) (Chae et al., 1999; Usui et al., 1999); Prickle (Pk), a LIM domain protein (Tree, 2002); and Van Gogh (Vang), also called Strabismus (Stbm) (Taylor et al., 1998; Wolff and Rubin, 1998). However, there is no direct evidence for a graded extracellular signal controlling PCP in *Drosophila*. Some experiments suggest instead that a presently undefined cell-to-cell mechanism propagates the PCP signal (Lawrence et al., 2004; Ma et al., 2003; Matakatsu and Blair, 2004; Strutt, 2002; Yang et al., 2002). The redistribution of the PCP core group proteins in the wing is not well understood and several mechanisms can be envisioned, but the result of the polarization signal is that Fz and the other core-group proteins are selectively redistributed to one or both sides of the cell. Fz and Dsh relocalize to the distal side of the cell (Axelrod, 2001; Strutt, 2001), Pk relocalizes to the proximal side, and Fmi is relocalized to both the proximal and distal sides of the cell (Tree, 2002; Usui et al., 1999). Redistribution of these molecules to the proximodistal (PD) boundaries creates a characteristic zig-zag pattern (Fig. 1B). In animals mutant for any of the core group proteins, the appropriate asymmetric relocalization of the remaining PCP proteins does not occur, and the wing hairs are aberrantly positioned and oriented (Fig. 1D). This loss of polarity is probably a direct effect of mislocalization of the core group proteins; however, there is evidence that is at odds with this model (Lawrence et al., 2004).

The PCP pathway is not a simple linear biochemical cascade as there is clear evidence for multiple branches. For example, after Fz relocalizes to the distal end of the cell, it regulates the non-muscle myosin regulatory light chain protein (MRLC; Mlc2 – FlyBase) and Myosin II through the small GTPase RhoA and Rho kinase (Rok) (Winter et al., 2001) (Fig. 1C). RhoA and Rok mutants show defects only in the number of wing hairs per cell, and not hair polarity errors. By comparison, mutants for the PCP core group show both wing hair number defects and inappropriate hair orientation (Fig. 1D). The current view is that Fz lies near the top of the PCP intracellular signaling and controls a branching biochemical pathway that organizes a polarized cell to project one distally oriented hair.

[1]Department of Molecular Cell and Developmental Biology, and Molecular Biology Institute, University of California at Los Angeles, Los Angeles, CA 90095, USA. [2]College of Physicians and Surgeons, Columbia University, New York, NY 10032, USA. [3]Department of Molecular Biology and Genetics, Cornell University, Ithaca, NY 14853-2703, USA.

*Present address: Center for Comparative Functional Genomics, NYU Department of Biology, New York, NY 10003-6688, USA
†Author for correspondence (e-mail: laski@mbi.ucla.edu)

Accepted 9 February 2006

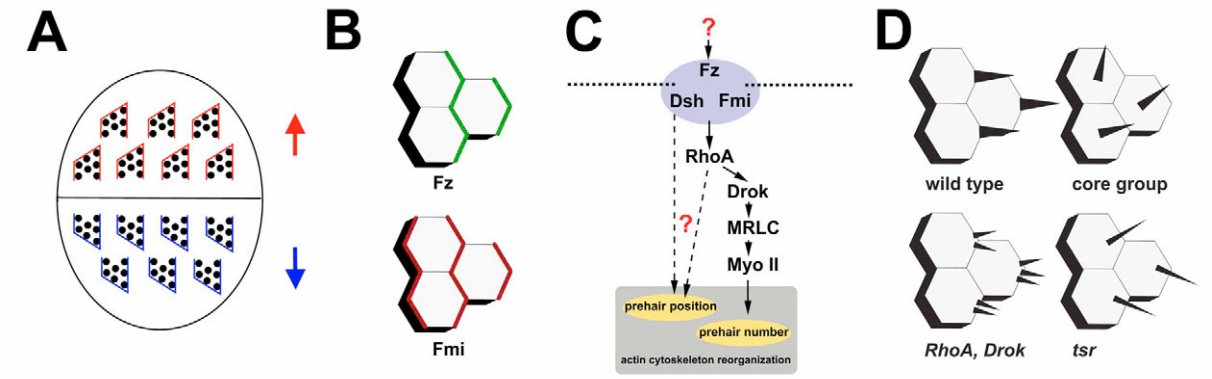

Fig. 1. Aspects of planar cell polarity. (**A**) In a wild-type eye, ommatidia are rotated uniformly above and below the dorsoventral equator. (**B**) Localization of the polarity cue. In wild-type wing cells, Fz is localized to the distal sides of cells, whereas Fmi is localized to both the proximal and distal sides of cells. (**C**) The basic PCP pathway that determines wing hair polarity. (**D**) Classes of PCP defects in the wing epithelium. In wild type, a single hair is secreted from the distal-most vertex of each cell. Mutations of the PCP core group genes (fz, fmi/stan, dsh, pk and vang/stmb) cause hairs to project from central locations and to have a non-distal orientation. RhoA and Rok mutants show multiple wing hairs projected from the distal side of a cell. The *tsr* mutants show a single wing hair that is projected in a non-distal orientation and is not centered through the distal-most vertex of a cell.

Tsr, the *Drosophila* homolog of cofilin (Cfl1)/ADF, belongs to a family of small actin-binding proteins (Bamburg, 1999). Cofilin/ADF binds filamentous actin, inducing a twist in the actin filament that enhances the rate of actin depolymerization from the pointed end (Carlier et al., 1997; Lappalainen and Drubin, 1997). Cofilin/ADF also severs F-actin, thereby increasing the number of actin filament barbed ends and increasing the rate of actin polymerization. Cofilin/ADF can therefore enhance both actin depolymerization and actin polymerization. The activity of Cofilin/ADF is regulated through phosphorylation (Arber et al., 1998; Yang et al., 1998). Cofilin/ADF is inactivated by Lim kinase 1, and reactivated by the phosphatases Slingshot (Niwa et al., 2002) and Chronophin (Gohla, 2005). As one of the main regulators of actin cytoskeleton remodeling, cofilin/ADF is required for many different processes in the cell, including: cell motility (Chen et al., 2001); cell polarity during migration (Dawe et al., 2003); endocytosis in yeast (Lappalainen and Drubin, 1997); axon guidance (Kuhn et al., 2000); and cytokinesis (Gunsalus et al., 1995). In this report, we show that Tsr is also required for the establishment of PCP and for the redistribution of the PCP core proteins Fz and Fmi to the PD boundary of cells during establishment of PCP in the wing. These data argue that actin remodeling is intimately involved in the polarization and protein redistribution mechanism.

MATERIALS AND METHODS

Molecular cloning and mutagenesis

Temperature sensitive *tsr* mutations were created by site-specific mutagenesis in the context of a 6.4 kb *tsr* genomic fragment. The oligonucleotides were: AATGTAAAAGATCTGATAGCGATGCTT for tsr^{V27Q} and CGGGAAGCCGTCGCTGCAGCACTCGCGGCCACCGA-CCGC for tsr^{139}. Mutations were amplified using the QuickChange kit (Stratagene), then subcloned in the context of the *tsr* 6.4 genomic rescue fragment (Chen et al., 2001) into the pP[C4cat] vector (Thummel et al., 1988). P[WHTG] is an abbreviation for P[w^+, *hsp70-tsr*^{gen}] in which the *tsr* protein-coding region is fused to the *hsp70* heat shock promoter and cloned into the pW8 vector. The *tsr* genomic fragment, P[WHTG], is 2548 bp, starting 101 bp upstream of the translation start site ATG and continuing to the *Pst*I site that is 385 bp downstream of the TAA stop codon.

The Limk cDNA LD15137 was obtained from the Berkeley *Drosophila* Genome Project and subcloned into the p[UAST] transformation vector (Brand and Perrimon, 1993). Disruption of the second Lim domain in human Lim kinase has previously been shown to increase its in vivo activity significantly (Edwards and Gils, 1999). Therefore, a mutated form of Limk (called $Limk^{\Delta NgoMIV}$), was made by modifying p[UAST-$Limk^{15137}$] by restriction digestion with *Ngo*MIV, creating an in-frame deletion of amino acids A109 to A175 that removes a sizeable part of the second Lim domain.

Drosophila strains

To express thermosensitive forms of Tsr from transgenes in a background that lacks endogenous Tsr activity, the following crosses were conducted, using a transgene located on the X-chromosome or 3rd chromosome. *y* w^{67}, pP[C4cat –tsr^{V27Q}]^{2A}; $tsr^{\Delta 96}$ was crossed to *y* w^{67}, pP[C4cat-tsr^{139}]^{1C}; $tsr^{\Delta 96}$ and was created on the 3rd chromosome by crossing. *y* w^{67}; $tsr^{\Delta 96}$; pP[C4cat-tsr^{V27Q}]^5 was crossed to *y* w^{67}; $tsr^{\Delta 96}$pP[C4cat-tsr^{139}]^2. Additional PCP defects were observed with the line *w,* P[WHTG]; $tsr^{\Delta 96}$/*TSTL*. Fz localization was examine by crossing in the Fz-GFP transgene (Strutt, 2001). Limk was overexpressed in the dorsal wing blade with: *y* w^{67}; P[UAST-$Limk^{\Delta NgoMIV}$] (three independent lines) and the GAL4 driver: *y w*; P[GawB]ap^{md544}/*CyO*,[y^+] (Calleja et al., 1996).

Microscopy

Confocal

Fluorescent microscopy was performed at the CNSI Advanced Light Microscopy/Spectroscopy Shared Facility at UCLA. Images were acquired using Leica Confocal Software (Leica Microsystems, Heidelberg GmbH) and were analyzed using NIH ImageJ. Confocal images were adjusted to best show protein localization and F-actin structures. Owing to the variability of fluorescence with each fluorophore within a sample and genotype, the relative intensities of expression are not intended be compared between wild type and the tsr^{V27Q}/tsr^{139} mutant.

Bright field

Adult wings were rinsed in 100% ethanol, transferred to PBS, then transferred into Hoyer's medium for mounting. Slides were baked overnight at 65°C and examined on a Zeiss Axioskop.

Scanning electron microscopy

Adult cuticles were examined with a Hitachi S-2460N scanning electron microsope. Images were acquired using the Quartz PCI version 3 imaging management system.

Staging mutant wing development

The cross to obtain *y* $w^{67}tsr^{V27Q}$/*y* $w^{67}tsr^{139}$; $tsr^{\Delta 96}$/$tsr^{\Delta 96}$ flies (Fig. 2B) was performed at 18°C. The homozygous *tsr* mutants are weak and develop at a variable and slower rate than their heterozygous siblings. Therefore, in addition to staging the wings by measuring time after puparium formation

(APF), we also compared mutant wings with the wild-type control grown in parallel at 18°C, and by comparison of the structural features of mutant wings to controls grown at 25°C.

Antibodies and immunohistology

Mutant pupae were staged at 18°C. Pupal cases were cut across the top of the operculum, and then cut laterally two-thirds of the way down the ventral side. Pupae were then fixed for 1 hour or 24 hours in 5% formaldehyde in PBS at 4°C. The pupal case was gently torn off at the cut exposing the pupa, but leaving the ends of the wings restrained by the remaining pupal case. The membrane encasing the wing was torn near the wing hinge, and the wing was gently pulled out. Pupal wings were rinsed three times in PBT (1×PBS, 1% Tween 20); blocked in PBT (+2% BSA) for at least 30 minutes; incubated overnight in a 1/10 dilution of primary Fmi monoclonal antibody at 4°C; rinsed three times in PBT for 10 minutes; blocked in PBT (+2% BSA) for at least 30 minutes; and incubated in 1/1000 dilution of secondary antibody [goat anti-mouse conjugated Alexa Fluor 594 (Molecular Probes)] and in a 1/200 dilution of Phalloidin (Alexa Fluor 488) overnight at 4°C. Wings were rinsed three or four times in PBT and mounted with Vectashield (Vector Laboratories). An α-GFP antibody conjugated with Alexa-Fluor 488 (Molecular Probes) was used a 1/200 dilution to enhance visualization of Fz-GFP. The α-Arm monoclonal antibody (Riggleman et al., 1990) was used at a 1/10 dilution (Developmental Studies Hybridoma Bank, product N2 7A1).

RESULTS

tsr conditional alleles have a planar cell polarity mutant phenotype

Tsr is required for cytokinesis, reducing the usefulness of mosaic analysis experiments to determine its role during development. We therefore engineered and tested two different forms of *tsr* mutants that are sensitive to temperature: one type being thermo-labile proteins, the other a heat-shock inducible gene. We have previously shown that a transformed wild-type *tsr* genomic fragment (P[mini-w^+; tsr^+]) can rescue the lethality of homozygous $tsr^{\Delta 96}$ null mutants (Chen et al., 2001). Two thermolabile mutations, tsr^{139} and tsr^{V27Q}, were independently introduced into the *tsr*-coding region of P[mini-w^+; tsr^+]. First, we changed amino acids 139 through 143 from the sequence EEKLR to AAALA and called the corresponding allele tsr^{139}; this mutation mimics the temperature-sensitive *cof1-22* mutation of yeast Cofilin (Lappalainen et al., 1997) (Fig. 2A). Second, we changed amino acid 27 from valine to glutamine and called the corresponding allele tsr^{V27Q}, which created an additional temperature sensitive form of the protein (Fig. 2A). A heat-inducible form of the *tsr* gene was engineered by placing a genomic fragment containing the *tsr*-coding region under the transcriptional control of the *hsp70* inducible heat shock promoter; this construct was called P[WHTG] (see Materials and methods).

P-element transformants of either tsr^{V27Q} or tsr^{139} showed limited rescue of the lethality caused by the $tsr^{\Delta 96}$ null allele; however, when put in transheterozygous combination: tsr^{V27Q}/tsr^{139}; $tsr^{\Delta 96}$ (hereafter abbreviated as tsr^{V27Q}/tsr^{139}; Fig. 2B) there was a complete rescue of lethality when grown at 18°C. When grown at 25°C, only a few rare escapers of this genotype survived, which was indicative of the temperature-sensitive nature of these alleles (see Table 1). Interestingly, although the tsr^{V27Q}/tsr^{139} flies grown at 18°C had a relatively healthy appearance, over 90% showed clear PCP defects of the wing. An adult wild-type wing grown at 18°C shows the normal pattern of uniformly distally pointing hairs (Fig. 3A). The tsr^{V27Q}/tsr^{139} wing shows an abnormal pattern of non-distally pointing hairs (Fig. 3B). When grown at temperatures above 18°C, there was an increase in lethality and other non-PCP-related defects; hence, for this analysis tsr^{V27Q}/tsr^{139} flies were grown at 18°C. Tsr is probably required for many different processes during development. The observation that tsr^{V27Q}/tsr^{139} flies grown at 18°C were relatively healthy, but had a high incidence of PCP defects indicates that the PCP defect is more sensitive to a reduction of Tsr activity than to other defects caused by these *tsr* mutations.

P[WHTG] is a P-element insertion on the X chromosome capable (albeit at a low frequency) of rescuing the lethality of the $tsr^{\Delta 96}$-null allele without heat-shock treatment. The rescue was more efficient when flies are raised at a high temperature, such as 28°C. Rescued flies of genotypes P[WHTG]/P[WHTG]; $tsr^{\Delta 96}/tsr^{\Delta 96}$ and P[WHTG]/Y; $tsr^{\Delta 96}/tsr^{\Delta 96}$ showed extensive PCP defects (Fig. 3C-I): in adult wings, hairs did not uniformly point distally (Fig. 3C); in eyes, ommatidia showed random chirality and polarity (Fig. 3D); in the abdomen, fine hairs and bristles frequently had non-posterior orientations (Fig. 3E); leg bristles often showed non-distal orientations and displayed aberrant tarsal joints and joint duplications (Fig. 3F-H); and bracts, the small hair-like structures at the base of the bristle sockets, showed opposite orientations (Fig. 3I). Such defective tarsal segmentation phenotypes, although not an obvious PCP defect, also occur in a number of polarity mutants such as *fz*, *dsh* and *prickle* (Held et al., 1986) and are regarded as a PCP-associated phenotype. Male flies of genotype P[WHTG]/Y;

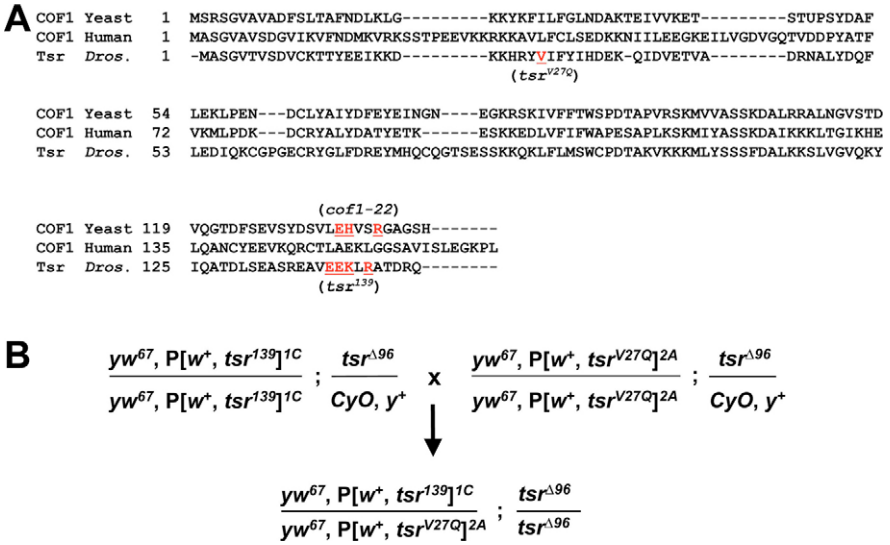

Fig. 2. Temperature-sensitive *tsr* mutantions. (**A**) Sequence comparisons of yeast, human and *Drosophila* cofilin sequences (Lappalainen et al., 1997). The cof1-22 mutation that gave a temperature sensitive phenotype in yeast is in red and denoted above the sequence. This mutation was used to predict and engineer a similar temperature-sensitive mutation in *Drosophila*, tsr^{139}, that is in red and denoted below the sequence. The position of the tsr^{V27Q} mutation is also indicated. (**B**) The cross generating tsr^{V27Q}/tsr^{139}; $tsr^{\Delta 96}$ progeny. The conditional alleles P[w^+, tsr^{139}] and P[w^+, tsr^{V27Q}] together rescued the lethality caused by the $tsr^{\Delta 96}$ mutation at the permissive temperature and allowed analysis of PCP defects in different tissues.

Table 1. Characteristics of the temperature sensitive *tsr*^{139} and *tsr*^{V27Q} mutations

Temperature	$\frac{tsr^{\Delta 96}}{tsr^{\Delta 96}}$	$\frac{P[w^+, tsr^{139}]^{1C}}{P[w^+, tsr^{139}]^{1C}} ; \frac{tsr^{\Delta 96}}{tsr^{\Delta 96}}$	$\frac{P[w^+, tsr^{V27Q}]^{2A}}{P[w^+, tsr^{V27Q}]^{2A}} ; \frac{tsr^{\Delta 96}}{tsr^{\Delta 96}}$	$\frac{P[w^+, tsr^{139}]^{1C}}{P[w^+, tsr^{V27Q}]^{2A}} ; \frac{tsr^{\Delta 96}}{tsr^{\Delta 96}}$
16°C	Lethal 1st instar	Pupal lethal adult escapers (0/73)	Pupal lethal adult escapers (0/66)	Adult progeny fertile females males escapers (25/231)
18°C	Lethal 1st instar	Pupal lethal adult escapers (5/913) two males	Pupal lethal adult escapers (1/1153) one male	Adult progeny fertile females males escapers (129/1481) two males
25°C	Lethal 1st instar	Few 2nd instar larvae	Few 2nd instar larvae	Few pupae
29°C	Lethal 1st instar	Lethal 1st instar	Lethal 1st instar	Lethal 1st instar

Transheterozygous adults for the mutations *tsr*^{V27Q} and *tsr*^{139} survive and are relatively healthy at 16°C and 18°C, but few animals survive to the late pupal stage at 25°C.

tsr$^{\Delta 96}$/*CyO, y*$^+$ appeared wild type; therefore, the phenotypes seen with P[WHTG]-rescued *tsr*$^{\Delta 96}$ homozygotes were not caused by the P-element insertion on the X chromosome, but rather resulted from a reduction in Tsr activity.

Polarity defects were also observed with the fine hairs of the notum. These hairs point to the posterior on wild-type nota, whereas many hairs adopted non-posterior orientations in a *tsr*^{V27Q}/*tsr*^{139} mutant (Fig. 3J). Occasionally, multiple hairs are observed (Fig. 3J, arrow); these abnormalities also occur in *fz* and *dsh* mutant animals (Krasnow et al., 1995; Wong and Adler, 1993). The *tsr*^{V27Q}/*tsr*^{139} genotype described above carried *tsr*^{V27Q} and *tsr*^{139} transgenes on the X chromosome; nearly identical phenotypes were observed when the *tsr*$^{\Delta 96}$ null allele was rescued by the transheterozygous combination of *tsr*^{V27Q} and *tsr*^{139} alleles on the 3rd chromosome (data not shown), indicating that the mutant phenotypes were not caused by a mutation induced by the X chromosome insertion of the P-element, but rather to reduced Tsr activity. This finding that compromised Tsr activity results in multiple defects that mimic those of mutants in the PCP pathway suggests that Tsr is a necessary component of this pathway.

Tsr is required for the distal orientation of wing hairs

In wild type, a single wing hair emerges from the distal vertex of each wing cell. Wing hairs in PCP mutants lose this distal orientation and initiate from the central region of a cell. To determine the location of *tsr*^{V27Q}/*tsr*^{139} prehair emergence, pupal wings were treated with phalloidin to visualize filamentous-actin-based structures. Distinct differences between wild-type and mutant wing cells were observed. Wild-type prehairs [~64 hours after puparium formation (APF) at 18°C] were first observed as F-actin accumulations at the distal side of cells (Fig. 4A). By contrast, the site of prehair initiation in *tsr*^{V27Q}/*tsr*^{139} wings was variable. In moderately to severely affected wings, prehairs were first observed as F-actin accumulations near cell centers (Fig. 4B, dot), or as long F-actin fibers that span from near cell centers to the distal side of cells (Fig. 4B, asterisk). During prehair emergence (over 64 hours APF at 18°C), wild-type prehairs were oriented along the PD axis and centered through the distalmost vertex of each cell (Fig. 4C). By contrast, *tsr*^{V27Q}/*tsr*^{139} prehairs were not oriented along the PD axis and had emerged from either side adjacent to the distal-most vertex

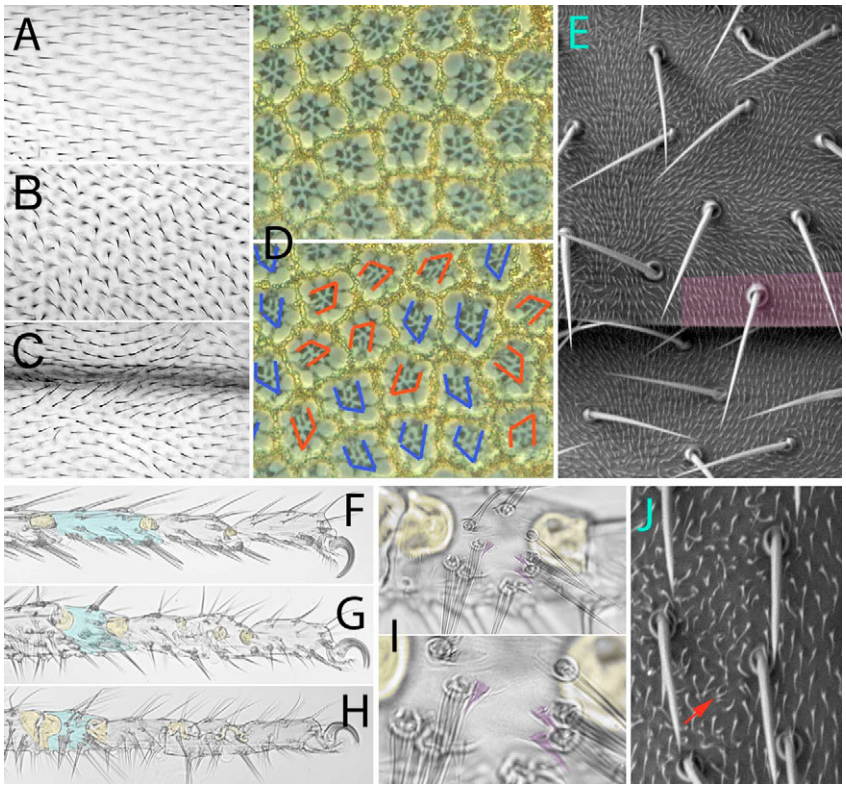

Fig. 3. *tsr* PCP defects in adult epithelia. *tsr*$^{\Delta 96}$ flies rescued by *tsr*^{139}/*tsr*^{V27Q} or P[WHTG] have PCP defects in several epithelia. (A-C) The wing (anterior is upwards and distal is rightwards). (**A**) Wild-type wings always have a uniform and distally pointing hair orientation; (**B**) *tsr*^{139}/*tsr*^{V27Q} wing hairs have a non-distal orientation; and (**C**) a P[WHTG] wing has hairs oriented in swirls or non-distally (not shown). (**D**) The eye. A thin section through a heat-shocked P[WHTG] eye shows a field of ommatidia that have randomly adopted polarities. (**E**) The abdomen. A P[WHTG] cuticle shows a random orientation of fine hairs. A region of hairs with wild-type orientation that points posteriorly is shaded. (**F-H**) The leg. A wild-type leg (F) shows normal segmentation and bristle pattern. Blue, tarsal segment 3; yellow, the correct joint position and polarity. P[WHTG] legs (G,H) have aberrant tarsal segments. Blue, the equivalent of tarsal segment 3 (from tibia); yellow, aberrant joints with duplications. At higher magnification (**I**), some P[WHTG] leg bristles show reversed polarity as do the 'bract-socket vectors' (Held et al., 1986). Bracts (purple) are fine hair-like structures at the base of each bristle: two bracts, one above the other, have the correct polarity: growing from the proximal side of the socket and point distally (to the right). The third bract has reversed polarity, growing from the distal side of the socket and points proximally. (**J**) The notum. A *tsr*^{139}/*tsr*^{V27Q} cuticle shows some of the fine hairs have lost the proper posterior-pointing orientation. Occasionally multiple hairs are observed (arrow).

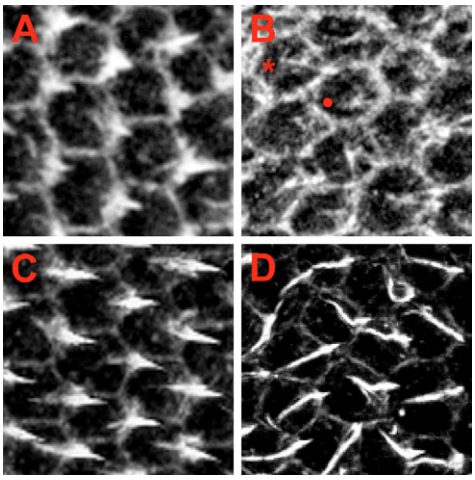

Fig. 4. Prehair emergence in pupal wings with reduced Tsr activity. Confocal images of wild-type and tsr mutant pupal wings stained with phalloidin. Anterior is upwards; distal is towards the left. (**A**) A wild-type wing shows prehairs initiating as accumulations of F-actin near or at the distal-most vertex of each cell. (**B**) A similarly staged tsr^{139}/tsr^{V27Q} wing shows prehairs initiated as F-actin accumulations located centrally (dot) or as elongated F-actin structures (asterisk). (**C**) An older wild-type wing shows prehairs centered over distal cell vertices. (**D**) A similarly staged tsr^{139}/tsr^{V27Q} wing shows prehairs with abnormal orientations that are similar to the pattern of hairs of the adult wing (Fig. 2B). tsr^{139}/tsr^{V27Q} prehairs are longer, thinner and extend non-distally.

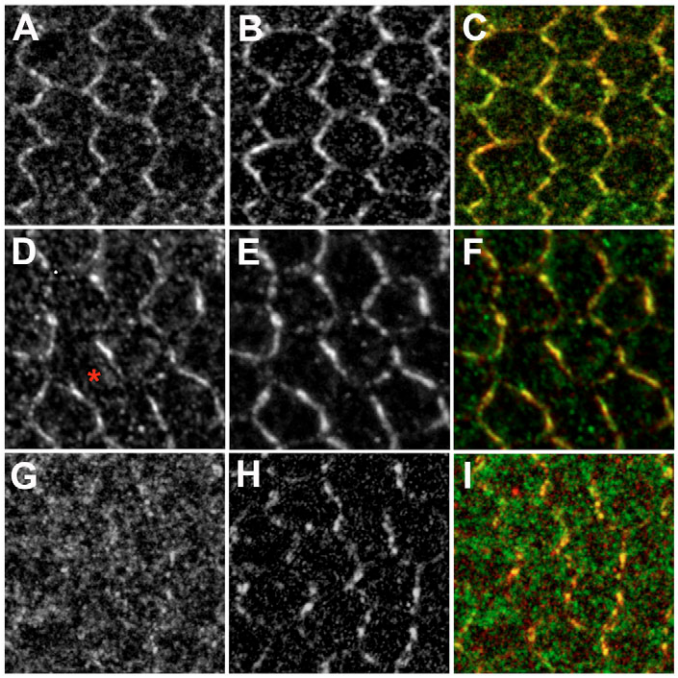

Fig. 5. Fz-GFP and Fmi are mislocalized in tsr mutant wings. Shown are: Fz-GFP (A,D,F); Fmi (B,E,G); and merged images of Fz-GFP in green and phalloidin-stained F-actin in red (C,F,I). (**A-C**) A wild-type wing, prior to prehair emergence aged greater than 48 hours APF at 18°C. Fz-GFP and Fmi are asymmetrically localized in a zigzag pattern at the PD boundary. The merged image shows Fz-GFP and Fmi colocalization. (**D-F**) A moderately affected tsr^{139}/tsr^{V27Q} wing of similar age shows an interrupted asymmetrical distribution of Fz-GFP. Fz-GFP is frequently missing from cell vertices and cell sides (asterisk). Similarly, Fmi shows an interrupted asymmetrical distribution. The merged image shows the extent of colocalization. (**G-I**) A severely affected tsr^{139}/tsr^{V27Q} wing shows that the recruitment of Fz-GFP to cell boundaries is largely lost, whereas Fmi is still enriched at cell boundaries where it shows an uneven and interrupted distribution. The merged image shows the zigzag pattern was interrupted.

of a cell (Fig. 4D). Although not completely penetrant, this phenotype was seen in the vast majority (>90%) of tsr^{V27Q}/tsr^{139} wings grown at 18°C. In addition to abnormal prehair emergence in tsr^{139}/tsr^{V27Q} mutant wings, the F-actin accumulation on apical cell surfaces was increased and variable when compared with the F-actin accumulation in wild-type wing cells (data not shown). As Tsr functions to depolymerize F-actin, an increase in F-actin concentration was expected and had been previously observed in *tsr* mutant ovaries (Chen et al., 2001).

Fz and Fmi do not correctly localize in *tsr* mutant wings

As Tsr appears to play a role in the PCP pathway, we asked whether the PCP core group members Fz and Fmi are properly localized in the tsr^{V27Q}/tsr^{139} mutant background. If correctly localized, this would suggest that Tsr acts downstream of these proteins. If incorrectly localized, Tsr would be required for the localization of these proteins. The temperature-sensitive tsr^{V27Q}/tsr^{139} mutant was grown at 18°C for this analysis. The rate of wing development in the tsr^{V27Q}/tsr^{139} mutants was variable, preventing us from using pupal age as the only accurate indication of the progress of wing development. Therefore, developmental stages were also determined by examining structural features of the pupal wing.

Fz and Fmi subcellular localizations were examined in wild type and in tsr^{V27Q}/tsr^{139} mutants by using the Fz-GFP transgene (Strutt, 2001) in conjunction with an anti-GFP antibody, and an anti-Fmi antibody. In wild type, after 48-hours APF (18°C), Fz and Fmi redistribute asymmetrically to the proximodistal boundaries of cells, forming the characteristic zigzag pattern (Strutt, 2001) (Fig. 5A-C). A typical tsr^{V27Q}/tsr^{139} mutant wing (Fig. 5D-F) shows a Fz-GFP and Fmi zigzag pattern that is markedly uneven compared with wild type, with gaps in the localization pattern at cell vertices (Fig. 5D), and larger gaps in which either or both proteins were missing from an entire side of a cell (Fig. 5D, asterisk). In a tsr^{V27Q}/tsr^{139} wing with a more severe phenotype, Fz-GFP was almost completely delocalized and Fmi appeared clustered in aggregates at cell boundaries (Fig. 5G-I). These data show that Tsr is required for the proper localization of Fz-GFP and Fmi. Although the localization of these proteins was not totally abolished, it is likely that the incomplete penetrance of this phenotype is the result of the partial rescue of the $tsr^{\Delta 96}$ null allele by the hypomorphic alleles tsr^{V27Q} and tsr^{139}. We anticipate that Fz-GFP and Fmi localization would be completely abolished in a stronger *tsr* mutant background; however, we are unable to verify this expectation because a further reduction of Tsr activity, such as raising tsr^{V27Q}/tsr^{139} flies at a temperature above 18°C, results in non-PCP defects that prevent data interpretation. These defects include abnormal cell size and shape, and abnormal accumulations of F-actin on apical cell surfaces (Table 1).

In wild type, at ~64 hours APF (18°C), Fz-GFP and Fmi distributions were enriched at the PD boundaries, and prehairs had emerged at the distal-most cell vertices (Fig. 6A-D). At a similar developmental stage, in tsr^{V27Q}/tsr^{139} wing cells of a moderately affected wing, both the Fz-GFP and Fmi protein distributions were

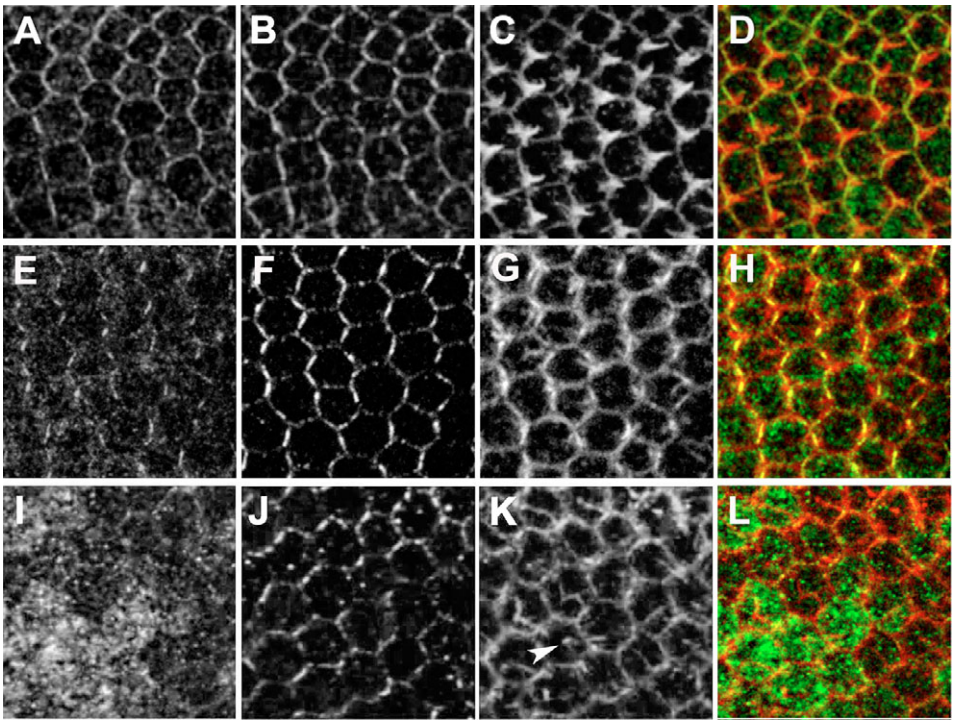

Fig. 6. Prehairs do not initiate from the correct location in *tsr* mutant wings. Fz-GFP (A,E,I); Fmi (B,F,J); F-actin (C,G,K); and merged images of Fz-GFP in green and phalloidin-stained F-actin in red (D,H,L). (**A-D**) A wild-type wing during prehair initiation aged ~64 hours APF at 18°C. Fz-GFP and Fmi show the characteristic asymmetrical distribution at the PD boundaries. F-actin accumulations show a single prehair centered at the distal-most vertex of each cell (C). The merged image shows the overlay of Fz-GFP (green) and F-actin (red) localization. (**E-H**) A moderately affected tsr^{139}/tsr^{V27Q} wing of a similar age shows a Fz-GFP distribution that was interrupted at the distal cell boundaries. (E) Fz-GFP accumulated unevenly and was missing from some cell boundaries. (F) Similarly, Fmi shows an uneven distribution at PD cell boundaries. (G) The F-actin accumulation shows prehairs were not centered through the distal vertices; few were extended. (H) The merged image. (**I-L**) tsr^{139}/tsr^{V27Q}, a severely affected wing shows that Fz-GFP is not enriched at PD boundaries and the Fmi distribution at PD boundaries is uneven showing puncti of strong staining alternating with gaps in the staining pattern. Phalloidin-stained F-actin (K) shows prehairs abnormally formed near cell centers (arrowhead). The merged image shows the extent of Fz-GFP delocalization.

in an uneven and gapped pattern, or were missing from a cell side, and prehairs had initiated from non-distal locations (Fig. 6E-H). In a more severely affected wing, Fz-GFP was almost completely delocalized; Fmi was not localized in the characteristic zigzag pattern; and prehairs had initiated aberrantly from central locations (arrowhead) (Fig. 6I-L, respectively). The loss of Fz-GFP localization from the PD boundary and the appearance of centralized sites of prehair initiation suggests that Tsr activity is required for the asymmetric distribution of Fz.

In wild type at greater than 66 hours APF (18°C), prehairs have emerged and the asymmetric distribution of Fz-GFP and Fmi is less apparent, becoming more symmetrically arrayed around the cell circumferences (Fig. 7A-C). At a similar developmental stage in tsr^{V27Q}/tsr^{139} wing cells, both the Fz-GFP and Fmi distributions were uneven and discontinuous, with regions of highly elevated protein concentration alternating with areas devoid of either protein (Fig. 7E-F). There was frequent colocalization between the Fz-GFP and Fmi proteins, suggesting that these proteins are closely associated (Fig. 7H). tsr^{V27Q}/tsr^{139} prehairs frequently passed through the region of highest Fz-GFP/Fmi accumulation in 68% of cells counted (Fig. 7G,H,H′; data not shown), suggesting that these accumulations present an orienting cue for the prehair outgrowth. Further, these data suggest that the *tsr* PCP wing defect is the result of a mislocalization of the Fz/Fmi signal and not due to an inability of the prehair to orient towards that signal.

Armadillo correctly localizes in *tsr* mutant wings

As a control, we investigated the localization pattern of Armadillo (Arm) in tsr^{139}/tsr^{V27Q} pupal wings. Mutations in *arm* have no direct effect on PCP signaling (Axelrod et al., 1998; Boutros et al., 1998); however, Arm is linked at the adherens junction to the cytoskeleton and is therefore a marker for the general organization of the actin cytoskeleton. Pupal wings were double stained for Arm and Fmi localization. There were no obvious differences between wild type and the *tsr* mutant prior to the asymmetric relocalization of the core group proteins to the PD boundary of cells (data not shown). Once Fmi was redistributed to form the zigzag pattern in wild type, the Arm distribution remained in the characteristic honeycomb pattern (see Fig. S1A,B in the supplementary material). In *tsr* mutant wings of similar age, the Fmi distribution appeared disrupted, but the Arm distribution remained in the characteristic honeycomb pattern (see Fig. S1C,D in the supplementary material). Later during development, after the wild-type Fmi zigzag pattern was no longer prominent, the Arm protein had disappeared; however, in tsr^{V27Q}/tsr^{139} wings of similar age, the Arm protein and pattern persisted (data not shown). This difference occurred well after wing hair polarity had been established. Therefore, the *tsr* PCP phenotype is not the result of a general disorganization of the actin cytoskeleton; rather, our findings are consistent with a direct role for *tsr* in PCP specification.

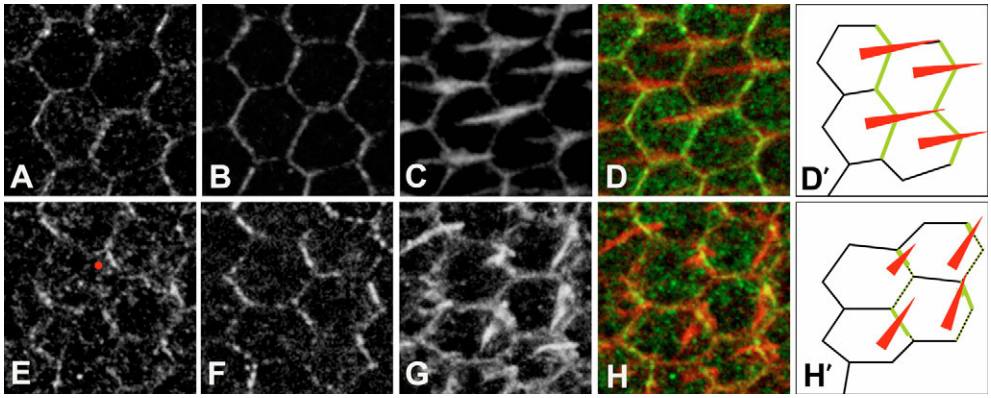

Fig. 7. Prehairs are oriented towards the highest accumulation of Fz-GFP and Fmi in *tsr* mutant wings. Shown are: Fz-GFP (A,E); Fmi (B,F); F-actin (C,G); and merged images (D,H; schematics of merged images D′,H′). (**A-D**) Prehairs in a wild-type wing aged ~66 hours APF at 18°C. Fz-GFP and Fmi shows the characteristic asymmetrical distribution at the PD boundaries; the zigzag pattern has begun to lose polarity at this stage. F-actin accumulation shows a single prehair pointing distally and aligned with the distal-most vertex of each cell. The merged image shows the overlay of Fz-GFP and F-actin localization. (**E-H**) Shown is a similarly aged tsr^{139}/tsr^{V27Q} wing. Fz-GFP distribution is interrupted at the distal cell-cell boundaries and accumulates more densely at some cell boundaries (E, dot). Similarly, Fmi is unevenly distributed at PD boundaries. The F-actin accumulation shows prehairs have non-distal orientations and are not aligned through the distal-most vertices. Prehairs appear to have emerged through the PD boundary at the point of a dense accumulation of Fz-GFP and Fmi (H,H′).

Overexpressing Lim kinase causes defects in planar cell polarity

Our experiments with *tsr* alleles suggested that regulation of the actin cytoskeleton has a crucial role in PCP and the appropriate localization of at least two of the PCP core group proteins. To verify this conclusion, we manipulated this pathway in a different manner by using *Drosophila* Limk, which phosphorylates ADF/cofilin thereby inhibiting its activity (Ohashi et al., 2000). Overexpression of a wild-type form of Limk showed only a weak mutant phenotype (at 23°C; data not shown). Therefore, an activated form of Limk ($Limk^{\Delta NgoMIV}$) was engineered by deleting a region of the second Lim domain (Edwards and Gils, 1999) and was expressed under Gal4-UAS transcriptional control (Brand and Perrimon, 1993). $Limk^{\Delta NgoMIV}$ was expressed in the dorsal wing blade using the *apterous* Gal4 (*ap*-Gal4) driver (Calleja et al., 1996), and the resulting phenotypes were found to be temperature sensitive. At 28°C, all the progeny died; at 25°C most animals died as pupae, but the few escapers had severe wing defects (data not shown). At 23°C, the progeny were fully viable. Approximately 10% of the progeny had wings that showed a whorled PCP pattern that is similar to the *fz* class of mutants (Fig. 8A), in which hairs tend to point in generally the same direction as their neighbors, while a majority of the progeny had wing hairs that frequently point in orientations independent of their neighbors (Fig. 8B). Examination of phalloidin stained UAS-$Limk^{\Delta NgoMIV}$/ap-Gal4 pupal wings showed that the PCP defects were limited to regions where the *ap* promoter is active, that is, on the dorsal wing blade (Fig. 8C, right panel). On the ventral wing blade, prehairs initiated as wild type from the distal-most vertices (Fig. 8D, left panel). Prehairs on the ventral wing blade had initiated aberrantly and were not centered (Fig. 8D, right panel), which is similar to the pattern of the tsr^{V27Q}/tsr^{139} mutant (Fig. 8E). Animals grown at 21°C showed no defects. Thus, by compromising the actin depolymerization pathway with an independent molecular tool, we were able to phenocopy the effects on PCP seen with the *tsr* mutant.

DISCUSSION

Using different methods of downregulating Tsr protein activity, either by expressing thermo-labile forms of the Tsr protein or by overexpressing its inhibitor Limk, we have shown that the actin remodeling pathway is required for the correct decoding of extracellular gradients into PCP. The question to be addressed is whether PCP is disturbed indirectly because the cells are generally compromised, or whether remodeling of the actin cytoskeleton instead plays a direct and specific role in transducing positional information in the cells. The following points strongly favor the latter interpretation:

(1) Reorganization of the actin cytoskeleton is required for the formation of hairs and bristles (Wong and Adler, 1993). However, the phenotypes we describe, cells produced these structures in a form that is close to wild type in appearance, yet the location and orientation of these structures are significantly altered. Morphogenesis of the eye also requires the active migration of cells, which requires the reorganization of the actin cytoskeleton. Yet, in the *tsr* mutant examined, the only defect in the ommatidia was of polarity.

(2) PCP defects have been observed in different tissues, including the wing, thorax, leg, abdomen and eye. One might expect PCP phenotypes in one tissue or another if cells were just generally compromised, but the universality of the effect argues for a PCP-specific effect.

(3) The PCP pathway directs tissue polarity in both the wing and eye, yet after PCP cues are established, the morphogenetic events that follow are very different. In the wing, PCP is manifest by the secretion of a single hair from a specific location in a cell. In the eye, PCP is manifest by the inter-communication of developing photoreceptor cells to direct specific cell fates. Thus, the *tsr* mutations affect two distinctly different mechanisms of development. This strongly suggests *tsr* acts at a point of the PCP pathway common in both the wing and eye, rather than at the level of the distinct morphogenetic events that follow.

(4) *tsr* mutants have aberrant tarsal segmentation that is characteristic of PCP mutants (Held et al., 1986). Thus, even the associated PCP effects are phenocopied in *tsr* mutants.

The above arguments highlight the strong genetic association between *tsr* and the PCP pathway, from which we infer that actin remodeling is a key step in the PCP generating mechanism. This is consistent with the work of Turner and Adler, whose data suggested that the actin cytoskeleton is important for the generation of wing hair polarity (Turner and Adler, 1998). Fz is the primary receptor for the PCP signal, and Fmi is at the top of the pathway required for the asymmetric redistribution of the PCP core proteins within the cell (Bastock et al., 2003). The molecular

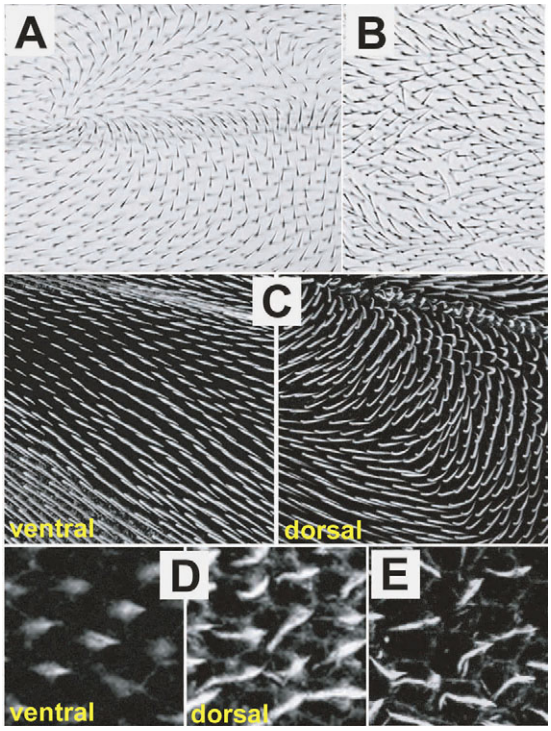

Fig. 8. Overexpression of a constitutively active Limk results in wing PCP defects. The activated Limk protein was expressed using an ap-Gal4 promoter construct that only expresses on the dorsal wing blade. Transgenic flies grown at 23°C survive and show defects with wing hair polarity similar to those seen in *fz* class wings (**A**), or have wing hairs that show a more chaotic wing hair orientation pattern (**B**). (**C**) A pupal wing, treated with phalloidin, on which the ventral surface hairs are oriented correctly (left panel), but hairs on the dorsal surface show the PCP defect (right panel). (**D**) A pupal wing with prehairs emerging correctly from the distal-most vertices on the ventral blade (left panel), while the dorsal blade (right panel) shows a phenotype similar to the tsr^{139}/tsr^{V27Q} mutant (**E**).

mechanisms required for this redistribution are not known. The above data strongly suggest that actin remodeling is involved in the stable redistribution of the core proteins. Possible mechanisms include: (1) that some of the core group proteins are transported on actin filaments; (2) that some core group proteins are bound to the actin cytoskeleton and actin depolymerization is required to release these proteins to allow their redistribution; (3) that redistribution of the core proteins occurs via an endocytosis/exocytosis pathway and actin reorganization is required for this process [cofilin is required for endocytosis in yeast (Lappalainen and Drubin, 1997)]; or (4) that actin filaments are required to stabilize the localized core group proteins, similar to the way actin filaments are required to stabilize localized phosphatidylinositol [PtdIns(3,4,5)P_3] in polarized migrating neutrophils (Wang et al., 2002). As Fz is the hierarchical organizer of the process, our results suggest that the actin remodeling pathway is an early target of Fz-mediated PCP signaling. We propose the following model. First, an extracellular gradient or a cell-to-cell mechanism activates the uniformly distributed Fz receptor (Adler et al., 1997; Strutt, 2001). Second, a graded activation of Fz across the cell engages Tsr-dependent actin reorganization that in turn leads to the asymmetric accumulation of Fz and associated core proteins by one of the molecular mechanisms described above. Third, the clustered Fz molecules send a high-level signal resulting in the reorganization of actin filaments into the future hair or bristle.

Although our data focus on the role of cofilin/ADF, other factors required for reorganization of the actin cytoskeleton would be expected to be required for establishment of PCP. The small GTPase Rho is a known regulator of the actin cytoskeleton and is regulated by Fz signaling. During wing hair formation, a signal transduction cascade from RhoA to Rok to MRLC to Myosin II is required to limit the formation of just a single wing hair per cell (Winter et al., 2001) (Fig. 1C). Interestingly, Rho kinase is a known regulator of cofilin/ADF that acts through Limk (Maekawa et al., 1999). However, the *tsr* mutant phenotypes described in this study are not consistent with a defect in the Rok branch of the pathway alone, as Tsr mutations affect wing hair orientation, not the number of wing hairs. In addition, Tsr is required for the proper redistribution of Fz and Fmi to the PD boundary of cells, whereas no requirement for RhoA and Rok has been demonstrated.

We thank Tadashi Uemura for the anti-Fmi antibody and the Bloomington Stock Center for numerous fly lines. We especially thank Jeronimo Ribaya for first identifying the *tsr* PCP phenotype and Dorothea Godt for thoughtful discussion. We also thank Madhuka Ranmuthu and Marina Stavchanskiy for technical assistance, and Lisolette L. Fessler for wing dissection assistance. Grants from the National Institutes of Health to F.A.L., A.T. and M.L.G. supported this work.

Supplementary material

Supplementary material for this article is available at http://dev.biologists.org/cgi/content/full/133/9/1789/DC1

References

Adler, P. N. (2002). Planar signaling and morphogenesis in Drosophila. *Dev. Cell* **2**, 525-535.

Adler, P. N., Krasnow, R. E. and Liu, J. (1997). Tissue polarity points from cells that have higher Frizzled levels towards cells that have lower Frizzled levels. *Curr. Biol.* **7**, 940-949.

Arber, S., Barbayannis, F. A., Hanser, H., Schneider, C., Stanyon, C. A., Bernard, O. and Caroni, P. (1998). Regulation of actin dynamics through phosphorylation of cofilin by LIM-kinase. *Nature* **393**, 805-809.

Axelrod, J. D. (2001). Unipolar membrane association of Dishevelled mediates Frizzled planar cell polarity signaling. *Genes Dev.* **15**, 1182-1187.

Axelrod, J. D., Miller, J. R., Shulman, J. M., Moon, R. T. and Perrimon, N. (1998). Differential recruitment of Dishevelled provides signaling specificity in the planar cell polarity and Wingless signaling pathways. *Genes Dev.* **12**, 2610-2622.

Bamburg, J. R. (1999). Proteins of the ADF/Cofilin family: essential regulators of actin dynamics. *Annu. Rev. Cell Dev. Biol.* **15**, 185-230.

Bastock, R., Strutt, H. and Strutt, D. (2003). Strabismus is asymmetrically localised and binds to Prickle and Dishevelled during Drosophila planar polarity patterning. *Development* **130**, 3007-3014.

Boutros, M., Paricio, N., Strutt, D. I. and Mlodzik, M. (1998). Dishevelled activates JNK and discriminates between JNK pathways in planar polarity and wingless signaling. *Cell* **94**, 109-118.

Brand, A. H. and Perrimon, N. (1993). Targeted gene expression as a means of altering cell fates and generating dominant phenotypes. *Development* **118**, 401-415.

Calleja, M., Moreno, E., Pelaz, S. and Morata, G. (1996). Visualization of gene expression in living adult Drosophila. *Science* **274**, 252-255.

Carlier, M. F., Laurent, V., Santolini, J., Melki, R., Didry, D., Xia, G. X., Hong, Y., Chua, N. H. and Pantaloni, D. (1997). Actin depolymerizing factor (ADF/cofilin) enhances the rate of filament turnover: implication in actin-based motility. *J. Cell Biol.* **136**, 1307-1322.

Chae, J., Kim, M.-J., Goo, J. H., Collier, S., Gubb, D., Charlton, J., Adler, P. N. and Park, W. J. (1999). The *Drosophila* tissue polarity gene *starry night* encodes a member of the protocadherin family. *Development* **126**, 5421-5429.

Chen, J., Godt, D., Gunsalus, K., Goldberg, M. and Laski, F. A. (2001). Cofilin/ADF is required for cell motility during *Drosophila* ovary development and oogenesis. *Nat. Cell Biol.* **3**, 204-209.

Dawe, H. R., Minamide, L. S., Bamburg, J. R. and Cramer, L. P. (2003). ADF/Cofilin controls cell polarity during fibroblast migration. *Curr. Biol.* **13**, 252-257.

Edwards, D. C. and Gils, G. N. (1999). Structural features of LIM kinase that control effects on the actin cytoskeleton. *J. Biol. Chem.* **274**, 11352-11361.
Gohla, A., Birkenfeld, J. and Bokoch, G. M. (2005). Chrononphin, a novel HAD-type serine protein phosphatase, regulates dependent actin dynamics. *Nat. Cell Biol.* **1**, 21-29.
Gubb, D. and Garcia-Bellido, A. (1982). A genetic analysis of the determination of cuticular polarity during development in Drosophila melanogaster. *J. Embryol. Exp. Morphol.* **68**, 37-57.
Gunsalus, K. C., Bonaccorsi, S., Williams, E., Verni, F., Gatti, M. and Golberg, M. (1995). Mutations in *twinstar*, a *Drosophila* gene encoding a Cofilin/ADF homologue, result in defects in centrosome migration and cytokinesis. *J. Cell Biol.* **131**, 1243-1259.
Held, L. I., Duarte, C. M. and Derakhshanian, K. (1986). Extra tarsal joints and abnormal cuticular polarities in various mutants of *Drosophila melanogaster*. *Rouxs Arch. Dev. Biol.* **195**, 145-157.
Krasnow, R. E. and Adler, P. N. (1994). A single frizzled protein has a dual function in tissue polarity. *Development* **120**, 1883-1893.
Krasnow, R. E., Wong, L. L. and Adler, P. N. (1995). Dishevelled is a component of the frizzled signaling pathway in Drosophila. *Development* **121**, 4095-4102.
Kuhn, T. B., Meberg, P. J., Brown, M. D., Bernstein, B. W., Minamide, L. S., Jensen, J. R., Okada, K., Soda, E. A. and Bamburg, J. R. (2000). Regulating actin dynamics in neuronal growth cones by ADF/cofilin and rho family GTPases. *J. Neurobiol.* **44**, 126-144.
Lappalainen, P. and Drubin, D. G. (1997). Cofilin promotes rapid actin filament turnover *in vivo*. *Nature* **388**, 78-82.
Lappalainen, P., Fedorov, E. V., Fedorov, A. A., Almo, S. C. and Drubin, D. G. (1997). Essential functions and actin-binding surfaces of yeast cofilin revealed by systematic mutagenesis. *EMBO J.* **16**, 5520-5530.
Lawrence, P. A., Casal, J. and Struhl, G. (2004). Cell interactions and planar polarity in the abdominal epidermis of Drosophila. *Development* **131**, 4651-4664.
Ma, D., Yang, C. H., McNeill, H., Simon, M. A. and Axelrod, J. D. (2003). Fidelity in planar cell polarity signalling. *Nature* **421**, 543-547.
Maekawa, M., Ishizaki, T., Boku, S., Watanabe, N., Fujita, A., Iwamatsu, A., Obinata, T., Ohashi, K., Mizuno, K. and Narumiya, S. (1999). Signaling from Rho to the actin cytoskeleton through protein kinases ROCK and LIM-kinase. *Science* **285**, 895-898.
Matakatsu, H. and Blair, S. S. (2004). Interactions between Fat and Dachsous and the regulation of planar cell polarity in the Drosophila wing. *Development* **131**, 3785-3794.
Niwa, R., Nagata-Ohashi, K., Takeichi, M., Mizuno, K. and Uemura, T. (2002). Control of actin reorganization by Slingshot, a family of phosphatases that dephosphorylate ADF/cofilin. *Cell* **108**, 233-246.
Ohashi, K., Hosoya, T., Takahashi, K., Hing, H. and Mizuno, K. (2000). A Drosophila homolog of LIM-kinase phosphorylates cofilin and induces actin cytoskeletal reorganization. *Biochem. Biophys. Res. Comm.* **276**, 1178-1185.
Riggleman, B., Schedl, P. and Wieschaus, E. (1990). Spatial expression of the Drosophila segment polarity gene armadillo is posttranscriptionally regulated by wingless. *Cell* **63**, 549-560.
Strutt, D. I. (2001). Asymmetric localization of frizzled and the establishment of cell polarity in the Drosophila wing. *Mol. Cell* **7**, 367-375.
Strutt, D. I. (2002). The asymmetric subcellular localisation of components of the planar polarity pathway. *Semin. Cell Dev. Biol.* **13**, 225-231.
Taylor, J., Abramova, N., Charlton, J. and Adler, P. N. (1998). *Van Gogh*: A new *Drosophila* tissue polarity gene. *Genetics* **150**, 199-210.
Thummel, C. S., Boulet, A. M. and Lipshitz, H. (1988). Vectors for Drosophila P-element-mediated transformation and tissue culture transfection. *Gene* **74**, 455-456.
Tree, D. R., Shulman, J. M., Rousset, R., Scott, M. P., Gubb, D. and Axelrod, J. D. (2002). Prickle mediates feedback amplification to generate asymmetric planar cell polarity signaling. *Cell* **109**, 371-181.
Turner, C. and Adler, P. N. (1998). Distinct roles for the actin and microtubule cytoskeletons in the morphogenesis of epidermal hairs during wing development in Drosophila. *Mech. Dev.* **70**, 181-192.
Uemura, T. and Shimada, Y. (2003). Breaking cellular symmetry along planar axes in *Drosophila* and vertebrates. *J. Biochem.* **134**, 625-630.
Usui, T., Shima, Y., Shimada, Y., Hirano, S., Burgess, R. W., Schwartz, T. L., Takeichi, M. and Uemura, T. (1999). Flamingo, a seven-pass transmembrane Cadherin, regulates planar cell polarity under the control of Frizzled. *Cell* **98**, 585-595.
Vinson, C. R. and Adler, P. N. (1987). Directional non-cell autonomy and the transmission of polarity information by the frizzled gene of Drosophila. *Nature* **329**, 549-551.
Vinson, C. R., Conover, S. and Adler, P. N. (1989). A Drosophila tissue polarity locus encodes a protein containing seven potential transmembrane domains. *Nature* **338**, 263-264.
Wang, F., Herzmark, P., Weiner, O. D., Srinivasan, S., Servant, G. and Bourne, H. R. (2002). Lipid products of PI(3)Ks maintain persistent cell polarity and directed motility in neutrophils. *Nat. Cell Biol.* **4**, 513-518.
Wehrli, M. and Tomlinson, A. (1995). Epithelial planar polarity in the developing Drosophila eye. *Development* **121**, 2451-2459.
Winter, C. G., Wang, B., Ballew, A., Royou, A., Karess, R., Axelrod, J. D. and Luo, L. (2001). Drosophila Rho-associated kinase (Drok) links Frizzled-mediated planar cell polarity signaling to the actin cytoskeleton. *Cell* **105**, 81-91.
Wolff, T. and Rubin, G. (1998). *strabismus*, a novel gene that regulates tissue polarity and cell fate decisions in *Drosophila*. *Development* **125**, 1149-1159.
Wong, L. L. and Adler, P. N. (1993). Tissue polarity genes of Drosophila regulate the subcellular location for prehair initiation in pupal wing cells. *J. Cell Biol.* **123**, 209-221.
Yang, C. H., Axelrod, J. D. and Simon, M. A. (2002). Regulation of Frizzled by fat-like cadherins during planar polarity signaling in the Drosophila compound eye. *Cell* **108**, 675-688.
Yang, N., Higuchi, O., Ohashi, K., Nagata, K., Wada, A., Kangawa, K., Nishida, E. and Mizuno, K. (1998). Cofilin phosphorylation by LIM-kinase 1 and its role in Rac-mediated actin reorganization. *Nature* **393**, 809-812.
Zheng, L., Zhang, J. and Carthew, R. W. (1995). frizzled regulates mirror-symmetric pattern formation in the Drosophila eye. *Development* **121**, 3045-3055.